https://dx.doi.org/10.4314/dujopas.v10i2b.35
ISSN (Print): 2476-8316
ISSN (Online): 2635-3490
Dutse Journal of Pure and Applied Sciences (DUJOPAS), *Vol. 10 No. 2b June 2024*

A Study on Unsteady Magneto-Hydrodynamics (Mhd) Free Convective Flow Past a Vertical Oscillating Plate Through a Porous Medium in the Presence of Heat Source

Sufiyanu Muhammad Dakin-Gari*[1], M. N. Sarki[2], A. U. DakinGari[4], I. D.Yale.[2,3]

[1]Department of Mathematics,
Kebbi State Polytechnic,
Dakingari,
Nigeria.

[2]Department of Mathematics,
Kebbi State University of Science and Technology,
Aliero,
Nigeria.

[3]Department of Electrical, Telecommunication and Computer Engineering,
Kampala International University,
Western Campus,
Uganda.

[4]Department of Mathematics,
Federal University Birnin-Kebbi,
Nigeria.

Email: sufiyanumuhammad77@gmail.com

Abstract

This study investigate time dependent MHD natural convective flow past a vertical oscillating plate through a porous medium in the presence of heat source. The governing differential equations of the flow characteristics are solved numerically by using the implicit finite difference scheme. The results obtained for the velocity, temperature and concentration were analysed. The effects of different physical parameters appear on the present situation such as Prandtl number (Pr), Schmidt number (Sc), thermal Grashof number (Gr), mass Grashof number (Gc), radiation (R), magnetic field (M), Time (t) and Heat source (Q) were presented graphically and discussed in detail. It is observed that the fluid velocity significantly increases as the value of Grashof number (Gr), mass Grashof number (Gc), Permeability parameter (K) and Time (t) increased, while the opposite phenomenon is noticed for growing values of magnetic field parameter (M), Prandtl number (Pr), radiation parameter (R), Schmidt number (Sc) respectively.

Keywords: Magneto-hydrodynamics, convective flow, porous medium, heat source

Author for Correspondence

INTRODUCTION

The study of electrically conducting liquids, including plasma, salty water, electrolytes, and liquid metals, is known as magneto-hydrodynamics (MHD). Numerous engineering and industrial uses for this kind of fluid exist, including crystal formation, reactor cooling, magnetic drug targeting, MHD sensors, and power generation. MHD is dependent on the intensity of magnetic induction (Jawad *et al*., 2021). The experimental investigation of modern MHD flow in a laboratory was first carried out by Hartmann and Lazarus (1937).

Free convection flows through an oscillatory flow in the involvement of heat source through a porous medium has been a subject of growing interest of many researchers due to its wide spectrum of applications in geophysics, solid mechanics, ground water, hydrology, oil recovery, thermal insulation, heat storage and in the field of engineering Chitra and Suhasini (2018). In view of the many applications of MHD oscillatory heat transfer flows, Usman and Sanusi (2023) recently explored the effects of non-Newtonian nanofluid flows across a semi-infinite flat plate immersed in a porous medium on heat radiation, Soret and pressure terms. Bafakeeh *et al*. (2022) discussed the unsteady hydromagnetic oscillatory natural convective heat and mass transfer flow of a viscous and electrically conducting fluid passing through a vertical plate immersed in a permeable medium in the coexistence of chemical reactions and thermal radiation affected by Hall current and Soret factor. Alwawi *et al.* (2020) performed a study of the MHD natural convection of sodium alginate Casson nanoliquid in a solid sphere. Sharma *et al.* (2022) emphasized the analytical study of MHD oscillatory time-dependent free convective viscous incompressible dissipative flow passing through an upstanding channel entrenched with porous medium in the coexistence of heat generation and thermal radiation factors.

It is well known that oscillatory flows result in increased mass and heat transfer. One can achieve oscillating movement by having a solid body vibrate within a fluid or by having a fluid vibrate around a fixed object. While fluid vibration around a fixed object uses more energy, both methods accomplish the same thing. Oscillating flows have been extensively studied by many researchers and found to be widely used in a variety of applications in the aerospace industry and military fields, as well as in compact high-performance heat exchangers, piston engines, chemical reactors, pulsating burners, high-performance Stirling engines, and cryogenic refrigeration. Khalid *et al.* (2017) examined the free convection flow of micropolar fluids over an Oscillating vertical plate. Pradhan *et al.* (2017) investigated the unsteady free convection flow of a viscous incompressible polar fluid past a semi-infinite vertical porous moving plate. Krishna *et al.* (2019) explored the temperature and accumulation transport on the MHD flow over an unlimited the non-conducting perpendicular flat porous plate. Convective flow is a self-sustained flow with the effect of the temperature gradient was analysed by Noor *et al.* (2020). Alwawi *et al.* (2020) performed a study of the MHD natural convection of sodium alginate Casson nano liquid in a solid sphere. In a similar study, Fu and Tong (2017) numerically examined the influence of a transversely oscillating cylinder on the heat transfer from heated blocks in a plane duct flow. Bila *et al.* (2023) were interested in Heat Transfer Enhancement of MHD Natural Convection in a Star-Shaped Enclosure, Using Heated Baffle and MWCNT–Water Nano fluid. Pourgholam *et al.* (2015) conducted a numerical research to investigate the effect of a rotating and oscillating blade on heat transfer enhancement from the channel walls. Jahangiri and Delbari (2020) numerically studied the details of the flow and heat transfer in a mixing tank equipped with a helical single-blade mixer.

The rate of thermal distribution in flow is influenced by the rate of heat creation at the boundary. Numerous manufacturing applications, such as the creation of electronic chips and fire modeling, demonstrate this. Heat waves propagate according to both flow velocity and surface temperature. Consequently, there must be a noticeable temperature differential someplace in the system for thermal radiation to occur. As a result, many systems' heat generation and absorption are dependent on the system's temperature and surroundings and are not constant. As found in studies conducted by Nemati *et al.* (2021)] who accounted periodic magnetic field effect with heat generation/absorption for a Non-Newtonian fluid. Elsayed *et al.* (2022) presents the effects of heat generation absorption on boundary layer flow of Nano fluid for a stretching cylinder. Khan *et al.* (2022) who examined the variable heat source for unsteady stagnation-point flow of magnetized Oldroyd-B fluid. The impact of ohmic heating for a double diffusive Nano fluid flow for stretching cylinder is considered in the study conducted by Yasir *et al.* (2022). Also as found in the investigation conducted by Sheikholeslami (2022) for thermal solar system, the thermal performance was found to be incremented upon elevating heat absorption.

Increasing convective heat transmission by the movement of a solid mass serving as a heat s ource is another subgroup of active methods that has been the focus of numerous studies. Rahman and Tafti (2020) numerically investigated convection heat transfer augmentation in a system composed of an infinitesimally thin plate-fin with forced oscillation in the presence of an approaching flow. Amar *et al.* (2022) discussed the MHD heat transfer flow over a moving wedge with convective boundary conditions with the influence of viscous dissipation and internal heat generation/absorption. Sarhan *et al.* (2019) experimentally investigated the vibration effect of a rectangular flat plate on convective heat transfer from the plate in both horizontal and inclined positions. Hussain *et al.* (2022) discussed the effectiveness of nonuniform heat generation and thermal characterization of a carreau fluid flowing across a nonlinear elongating cylinder. Akcay *et al.* (2020) experimentally investigated the convection heat transfer from an oscillating vertical plate.

Studying unsteady MHD free convective flow past a vertical oscillating plate through a porous media in the presence of a heat source is the main goal of the current investigation. The implicit finite difference approach is used to solve the momentum, energy, and diffusion equations that controlled the flow. Graphs are used to calculate, debate, and illustrate the impacts of different physical parameters on fluid velocity, temperature, and concentration at the plates.

METHODOLOGY

Mathematical Formulations

The current work examined the unstable one-dimensional flow via a porous media and a heat source of a viscous, incompressible, electrically conducting, radiating fluid past a vertical oscillating plate. The x and y axes in the Cartesian coordinate system should be taken normal to the plate and vertically upward along the plate, respectively. The irregular movement of a viscous incompressible fluid, initially at rest, around an infinite vertical plate with a concentration of C'_{∞}' and a temperature of T_{∞}.in a fixed state for the entire point. Additionally, it is assumed that the fluid's concentration and temperature are the same on the plate. When time $t' > 0$, the plate begins to oscillate at frequency ω' inside its own plane, and its temperature rises to T_w and the concentration level near the plate is raised linearly with respect to time. A transverse magnetic field of uniform strength B_o is assumed to be applied normal to the plate. The viscous dissipation and induced magnetic field are assumed to be negligible.

The fluid is considered to be gray, absorbing/emitting radiation but a non-scattering medium. Under these assumptions, the equations governing the unsteady flow can be obtained as follows:

Momentum equation

$$\frac{\partial u'}{\partial t'} = v\frac{\partial^2 u'}{\partial y'^2} - \left(\frac{v}{k'} + \frac{\sigma B_o^2}{\rho}\right)u' + g\beta(T - T_\infty) + g\beta'(C' - C'_\infty) \quad (1)$$

Energy equation

$$\frac{\partial T'}{\partial t'} = \frac{K}{\rho c_p}\frac{\partial^2 T'}{\partial y'^2} - \frac{1}{\rho c_p}\frac{\partial q_r}{\partial y'} + \frac{Q'}{\rho c_p}(T - T_\infty) \quad (2)$$

Diffusion equation

$$\frac{\partial C'}{\partial t'} = D\frac{\partial^2 C'}{\partial y'^2} - K_1(C' - C'_\infty) \quad (3)$$

The corresponding initial and boundary conditions for the model are as follows:

$$\left\{\begin{array}{c} t' \le 0: u' = 0, T' = T'_\infty, C' = C'_\infty, for\ all\quad y', \\ t > 0: \left\{\begin{array}{c} u' = u_o\, cos\omega' t', T = T_w,\quad C' = C'_\infty + (C'_w - C'_\infty)At', at\ y' = 0 \\ u_o = 0,\ \ T \to T_\infty,\ \ C' \to C'_\infty,\quad as\ y' \to \infty \end{array}\right\} \end{array}\right\} \quad (4)$$

Where, respectively, $x'$and y' represent the dimensional distances parallel and perpendicular to the plate. T' is the thermal temperature inside the thermal boundary layer and C' is the corresponding concentration; σ is the electric conductivity; C_p is the specific heat at constant pressure; D is the diffusion coefficient; $q_r$is the heat flux; Q' is the dimensional heat absorption coefficient; and K is the chemical reaction parameter. The velocity components in the $x'$and y' directions are u' and v', respectively; g is the gravitational acceleration; ρ is the fluid density; β and β' are the thermal and concentration expansion coefficients; and K' is the Darcy permeability.

The local radiant q_r for the case of an optically thin gray gas is expressed by Muthucumuraswamy and Geetha (2013).

$$\frac{\partial q_r}{\partial y'} = -4a^*\sigma\left(T'^4{}_\infty - T'^4\right) \quad (5)$$

It is assumed that, the temperature differences within the flow are sufficiently small such that T'^4 may be expressed as a linear function of the temperature T'_∞.This is obtained by expanding T'^4 in a Taylor series about T'_∞ and neglecting higher-order terms, thus:

$$T'^4 \cong 4\,T'^3{}_\infty T - 3\,T'^4{}_\infty. \quad (6)$$

METHOD OF SOLUTION

We incorporate the following non-dimensional variables and parameters in order to solve the governing equations in dimensionless form:

$$\left\{\begin{array}{c} y = \frac{y'u_o}{v}, t = \frac{t'u_0^2}{v}, u = \frac{u'}{u_o}, \theta = \frac{T' - T'_\infty}{T'_w - T'_\infty}, Gc = \frac{g\beta^*(C' - C'_\infty)}{u_0^3}, \\ \vdots \\ Gr = \frac{g\beta v(T - T_\infty)}{u_0^3}, C = \frac{(C' - C'_\infty)}{C'_w - C'_\infty}, Pr = \frac{\mu C_p}{k},\ \ Sc = \frac{v}{D}, K = \frac{u_0^2 K_1}{v^2} \\ R = \frac{16a^* v^2\sigma\, T'^3{}_\infty}{u_0^2}, K_c = \frac{vK_1}{u_0^2}, M = \frac{\sigma B_o^2 v}{\rho u_0^2} \end{array}\right\} \quad (7)$$

The governing equations on using (9) into (1), (3), and using (5) - (8) into (2) reduce to

$$\frac{\partial u}{\partial t} = \frac{\partial^2 u}{\partial y^2} + Gr\theta + GmC - \left(\frac{1}{K} + M\right)u \quad (8)$$

$$\frac{\partial \theta}{\partial t} = \frac{1}{Pr}\frac{\partial^2 \theta}{\partial y^2} + \frac{1}{Pr}(R + Q)\theta \quad (9)$$

$$\frac{\partial C}{\partial t} = \frac{1}{Sc}\frac{\partial^2 C}{\partial y^2} - KrC \quad (10)$$

While the dimensionless initial and boundary conditions are

$$\left\{\begin{array}{l} t \le 0: u = 0, \theta = 0, C = 0 \quad at\ y \le 0 \\ t > 0: \left\{\begin{array}{l} u = 0, \theta = 1, \quad C = 1 \quad at\ y = 0 \\ u = 0, \quad \theta = 0, \quad C = 0, \quad at\ y = 1 \end{array}\right. \end{array}\right\} \quad (11)$$

Where Pr is the Prandtl number, Sc is Schmidt number, Gr is thermal Grashof number, Gc is mass Grashof number, M is magnetic field, K is porosity, R is the radiation and Q is heat source.

Numerical Solution

In the present study we have considered a uniform spacing in each coordinate direction. According to our consideration, Δx and Δy are constants, but it is not mandatory that Δx be equal to Δy. The grid points are identified by an index i which increases in the positive x -direction, and an index j, which increases in the positive y -direction. If (i, j) is the index of point P in Figure 1, then the point immediately to the right is designated as $(i + 1, j)$ and the point immediately to the left is $(i - 1,\ j)$. Similarly the point directly above is $(i + 1, j)$, and the point directly below is $(i - 1,\ j)$. The basic philosophy of finite difference method is to replace the derivatives of the governing equations with algebraic difference quotients. This will result in a system of algebraic equations which can be solved for the dependant variables at the discrete grid points in the flow field.

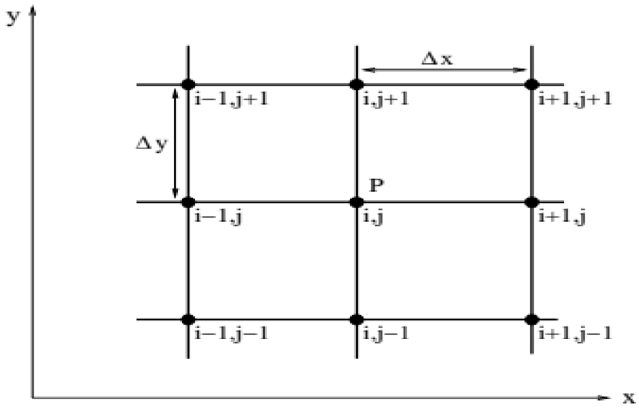

Figure 1: Implicit finite difference system grid

Equations (8), (9) and (10) are unsteady coupled non-linear partial differential equations and are to be solved under the initial and boundary condition of equation (11). However, exact or approximate solutions are difficult for these set of equations and hence were solved by the implicit finite difference scheme. The Implicit finite difference scheme of the differential terms in the governing equations (8), (9) and (10) are determines as;

$$\frac{\partial u}{\partial t} = \frac{U_i^{j+1} - U_i^j}{\Delta t}, \frac{\partial u}{\partial y} = \frac{U_i^{j+1} - U_i^j}{\Delta y}, \frac{\partial^2 u}{\partial y^2} = \frac{\left(U_{i-1}^{j+1} - 2U_i^{j+1} + U_{i+1}^{j+1}\right)}{\Delta y^2}, \frac{\partial \theta}{\partial t} = \frac{\theta_i^{j+1} - \theta_i^j}{\Delta t},$$

$$\frac{\partial \theta}{\partial y} = \frac{\theta_i^{j+1} - \theta_i^j}{\Delta y}, \frac{\partial^2 \theta}{\partial y^2} = \frac{\left(\theta_{i-1}^{j+1} - 2\theta_i^{j+1} + \theta_{i+1}^{j+1}\right)}{\Delta y^2}, \frac{\partial C}{\partial t} = \frac{C_i^{j+1} - C_i^j}{\Delta t}, \frac{\partial C}{\partial y} = \frac{C_i^{j+1} - C_i^j}{\Delta y},$$

$$\frac{\partial^2 C}{\partial C^2} = \frac{\left(C_{i-1}^{j+1} - 2C_i^{j+1} + C_{i+1}^{j+1}\right)}{\Delta y^2}. \quad (12)$$

Considering the implicit finite difference scheme of equation (12) and substitute into equations (8), (9) and (10) respectively.

$$\frac{U_i^{j+1} - U_i^j}{\Delta t} = \propto \frac{\left(U_{i-1}^{j+1} - 2U_i^{j+1} + U_{i+1}^{j+1}\right)}{\Delta y^2} + (1-\propto)\frac{\left(U_{i-1}^{j} - 2U_i^{j} + U_{i+1}^{j}\right)}{\Delta y^2} + Gr\theta_i^j + GmC_i^j - MU_i^j - K^{-1}U_i^j \quad (13)$$

The Implicit finite difference scheme of the equation (9), is solved as follows;

$$\frac{\theta_i^{j+1} - \theta_i^j}{\Delta t} = \frac{1}{Pr}\left[\propto \frac{\left(\theta_{i-1}^{j+1} - 2\theta_i^{j+1} + \theta_{i+1}^{j+1}\right)}{\Delta y^2} + (1-\propto)\frac{\left(\theta_{i-1}^{j} - 2\theta_i^{j} + \theta_{i+1}^{j}\right)}{\Delta y^2}\right] - \frac{1}{Pr}\left(R - Q\theta_i^j\right) \quad (14)$$

The Implicit finite difference scheme of the equation (10), is solved as follows;

$$\frac{C_i^{j+1} - C_i^j}{\Delta t} = \frac{1}{Sc}\left[\propto \frac{\left(C_{i-1}^{j+1} - 2C_i^{j+1} + C_{i+1}^{j+1}\right)}{\Delta y^2} + (1-\propto)\frac{\left(C_{i-1}^{j} - 2C_i^{j} + C_{i+1}^{j}\right)}{\Delta y^2}\right] - KrC_i^j \quad (15)$$

Following the implicit scheme, we obtained the following equations (16), (17) *and* (18) which will be computed in MATLAB and plot the corresponding graphs respectively.

$$-r_1U_{i-1}^{j+1} + (1+2r)U_i^{j+1} - r_1U_{i+1}^{j+1} = r_2U_{i-1}^j + (1-2r_2-r_3-r_4)U_i^j + r_2U_{i+1}^j + \Delta tGr\theta_i^j + \Delta tGmC_i^j \quad (16)$$

$$-r_1\theta_{i-1}^{j+1} + (Pr+2r_1)\theta_i^{j+1} - r_1\theta_{i+1}^{j+1} = r_2\theta_{i-1}^j + (Pr-2r_2+r_5)\theta_i^j + \Delta tR + r_2\theta_{i+1}^j \quad (17)$$

$$-r_1C_{i-1}^{j+1} + (Sc+2r_1)C_i^{j+1} - r_1C_{i+1}^{j+1} = r_2C_{i-1}^j + (Sc-2r_2-r_6Sc)C_i^j + r_2C_{i+1}^j \quad (18)$$

Where $r_1 = \frac{\propto \Delta t}{\Delta y^2}, r_2 = \frac{(1-\propto)\Delta t}{\Delta y^2}, r_5 = \Delta tQ, r_3 = \Delta tM, r_4 = \frac{\Delta t}{K} r_6 = \Delta tK,$

The mesh size along y- direction and time t-direction are Δy and Δt respectively while the index i refers to space y and j refers to time t . The finite difference equations (16), (17) and (18) at every internal nodal point on a particular n-level constitute a tridiagonal system of equations which are solved by using the Thomas algorithm.

RESULTS AND DISCUSSION

This study presented an investigation of MATLAB package and how it is been used for the coding of numerical solutions, to obtain the graphs and analysed the influence of several physical flow parameters such as thermal Grashof number (Gr), Prandtl number (Pr), Heat source (Q) parameters, mass Grashof number (Gc), radiation (R), magnetic field (M), porosity (K) and Schmidt number (Sc). These parameter values are static during the computations unless where otherwise stated. Pr = 0.70, Sc = 0.57, R= 0.10, M = 1, K = 1, Gr = 5, Gc = 5, Q = 1, and t = 0.2.

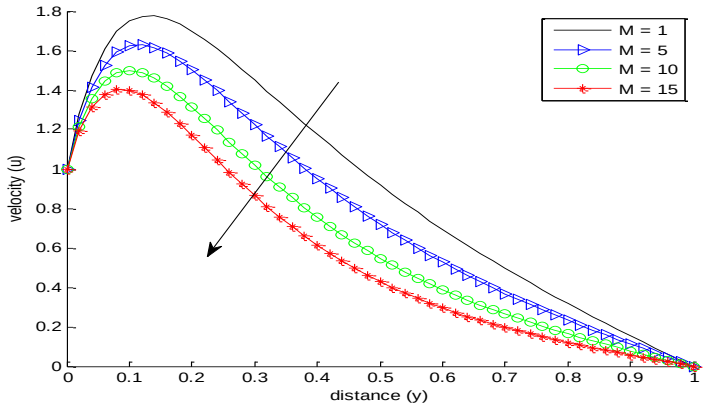

Figure 2 : influence of magnetic parameter (M) on velocity profile when Pr = 0.70, dt = 0.004, dy = 1/m, y = 0:dy:1, dy2 = 2.0*dy, t = 0.2, K = 1, Gr = 5, Gc = 5, Sc = 0.57, and R = 0.10.

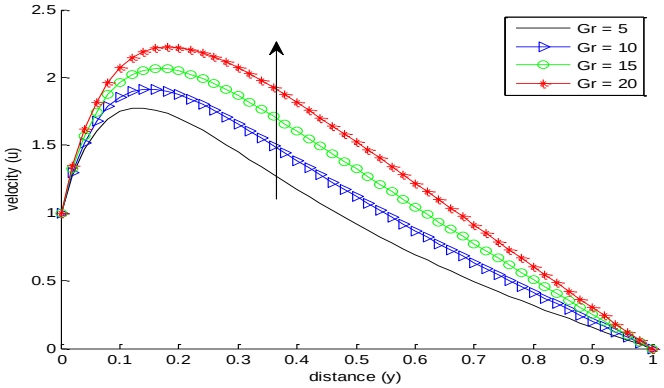

Figure 3: Effect of Grashof number (Gr) on velocity profile when Pr = 0.70, dt = 0.004, dy = 1/m, y = 0:dy:1, dy2 = 2.0*dy, t = 0.2, K = 1, Gc = 5, Sc = 0.57, R = 0.10 and M = 1

The effects of magnetic parameter (M = 1, 5, 10, 15) and thermal Grashof numbers (Gr = 5, 10, 15, and 20) on the velocity profiles are shown in Figures 2 and 3 above. Figure 2 illustrates how the presence of magnetic force causes a velocity drop as the magnetic field parameter increases. These forces may interact with the fluid, causing it to drag and maybe move. The fluid's velocity decreases because the magnetic field resists the fluid's motion. These result are in good agreement with the results obtained in case of Usman and Sanusi (2023). However, Figure 3 showed the reverse occurrence, showing that at a fixed value of other parameters, the fluid velocity increased with rising values of the thermal Grashof number.

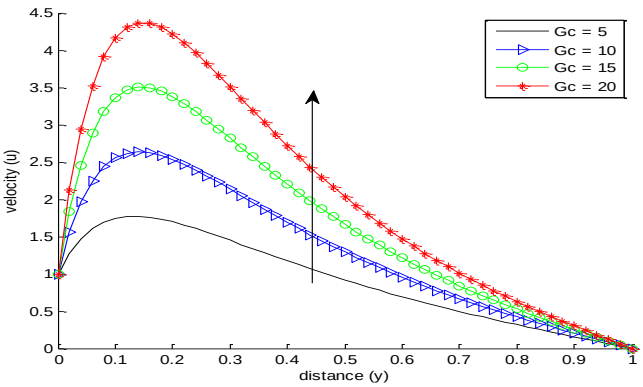

Figure 4: Effect of Mass Grashof number on velocity profile when Pr = 0.70, dt = 0.004, dy = 1/m, y = 0:dy:1, dy2 = 2.0*dy, t = 0.2, K = 1, Gr = 5, Sc = 0.57, R = 0.10, and M = 1

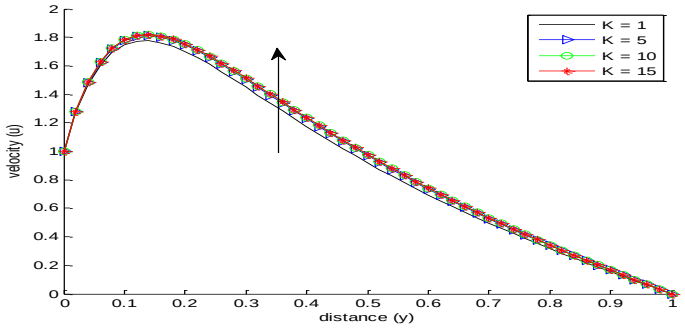

Figure 5: Effect of Porosity parameter (K) on velocity profile when Pr = 0.70, dt = 0.004, dy = 1/m, y = 0: dy: 1, dy2 = 2.0*dy, t = 0.2, K = 1, Gr = 5, Gc = 5, Sc = 0.57, R = 0.10, and M = 1

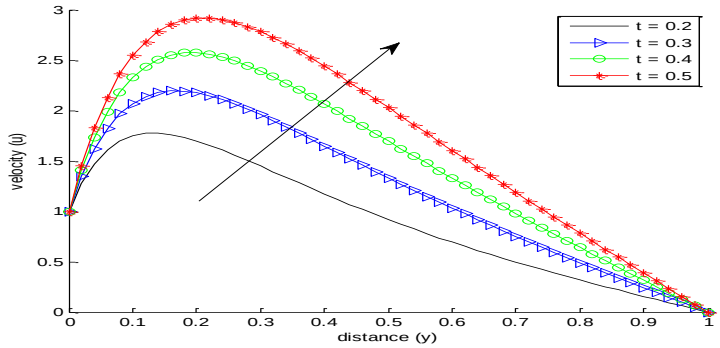

Figure 6: Effect of time (t) on velocity profile when Pr = 0.70, dt = 0.004, dy = 1/m, y = 0:dy:1, dy2 = 2.0*dy, K = 1, Gr = 5, Gc = 5, Sc = 0.57, R = 0.10, and M = 1.

The impact of the Mass Grashof number (Gr = 5, 10, 15, 20), Permeability parameter (K = 1, 5, 10, 15) and time (t = 0.2, 0.3, 0.4, 0.5) on velocity profiles is shown in Figure 4, 5 and 6. Figure 4, illustrates how the fluid velocity increased with increasing Mass Grashof number values for fixed values of other parameters. Figure 5 also shows how the fluid velocity increased significantly as Permeability parameter (K) values increased for fixed values of other parameters. This is because fewer obstacles to fluid flow exist in a more permeable medium. As a result, the fluid can pass through a porous material more readily and at greater speeds. Figure 6 further shows that, for a fixed value of other parameters, the fluid velocity increases with increasing time.

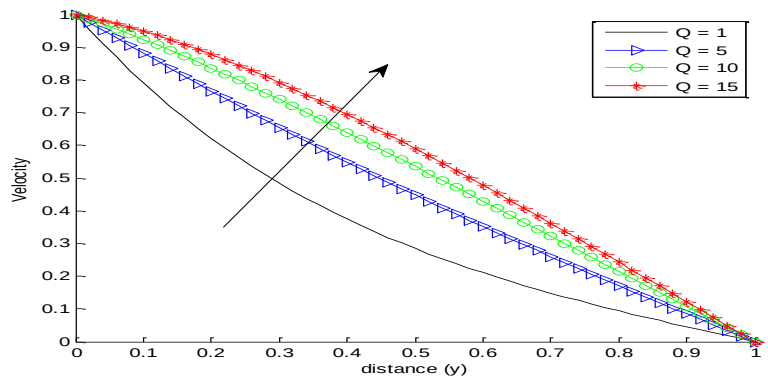

Figure 7: Effect of Heat source parameter on velocity profile when Pr = 0.70, dt = 0.004, dy = 1/m, y = 0:dy:1, dy2 = 2.0*dy, K = 1, Gr = 5, Gc = 5, Sc = 0.57, R = 0.10, and M = 1.

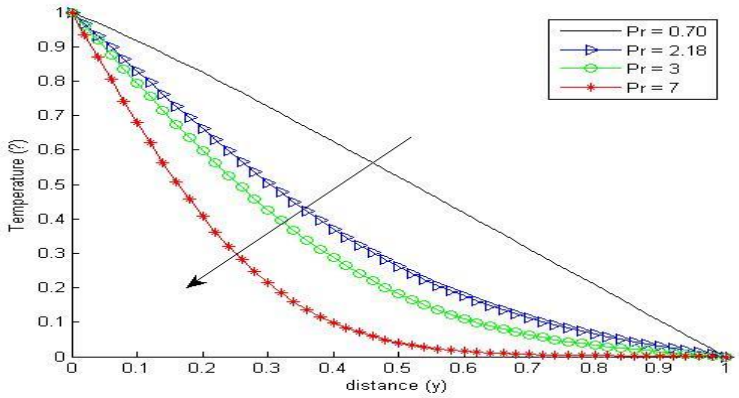

Figure 8: Effect of Prandtl number (Pr) on temperature profile when M = 1, dt = 0.004, dy = 1/m, y = 0:dy:1, dy2 = 2.0*dy, t = 0.2, Gr = 5, Gm = 5, Q = 1, R = 0.10, and Sc = 0.57.

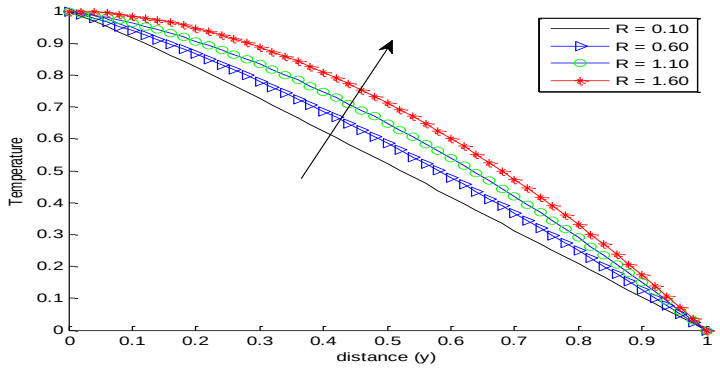

Figure 9: Effect of Radiation parameter (R) on temperature profile when M = 1, dt = 0.004, dy = 1/m, y = 0:dy:1, dy2 = 2.0*dy, Pr = 0.70 t = 0.2, Gr = 5, Gm = 5, Q = 1, and Sc = 0.57.

The impact of of heat source (Q = 1, 3, 7, 10), Prandtl number (Pr = 0.70, 2.18, 3.0, 7.0) and Radiation (R = 0.10, 0.60, 1.10, 1.60) parameters on the temperature profile are shown in Figure 7, 8, and 9. The graph in Figure 7 indicated that as the heat source parameter increases, the velocity of the fluid increases. The impact of changing the Prandtl number (Pr = 0.70, 2.18, 3.0, 7.0) on the temperature gradient is shown in Figure 8. The graph shows that when the Prandtl number increases, temperature decreases. This is physically true because a higher Prandtl number indicates that thermal diffusion is slower than momentum diffusion, leading to a thinner thermal boundary layer. Figure 9 depicts that the temperature increases with an increase in the radiation parameter. This is physically true because the temperature rises as the system absorbs more energy from radiation sources. The result establishes an excellent agreement with work of Sharma *et al.* (2022).

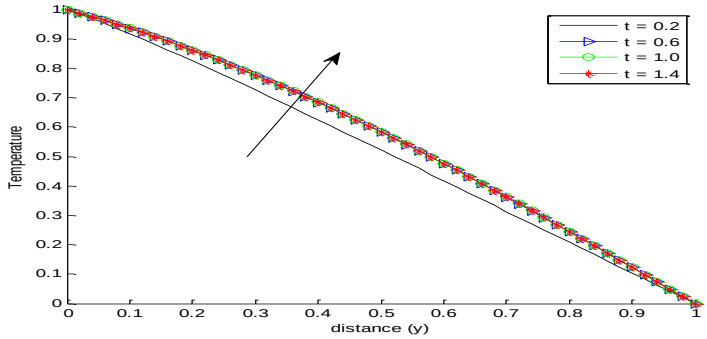

Figure 10: Effect of time (t) on temperature profile when M = 1, dt = 0.004, dy = 1/m, y = 0:dy:1, dy2 = 2.0*dy,t = 0.2, Gr = 5, Gm = 5, R = 0.10, and Sc = 0.57.

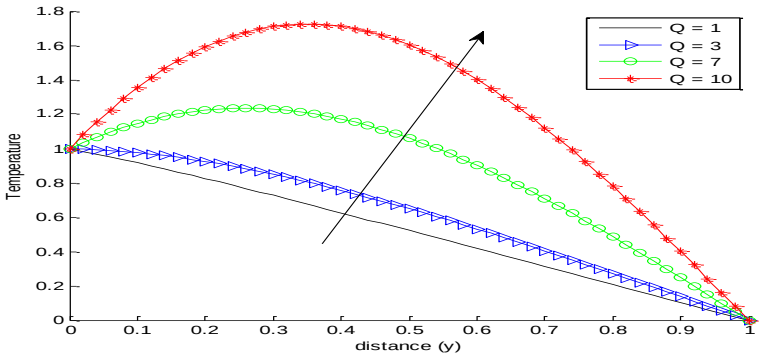

Figure 11: Effect of Heat source Parameter (Q) on temperature profile when M = 1, dt = 0.004, dy = 1/m, y = 0:dy:1, dy2 = 2.0*dy,t = 0.2, Gr = 5, Gm = 5, R = 0.10, and Sc = 0.57.

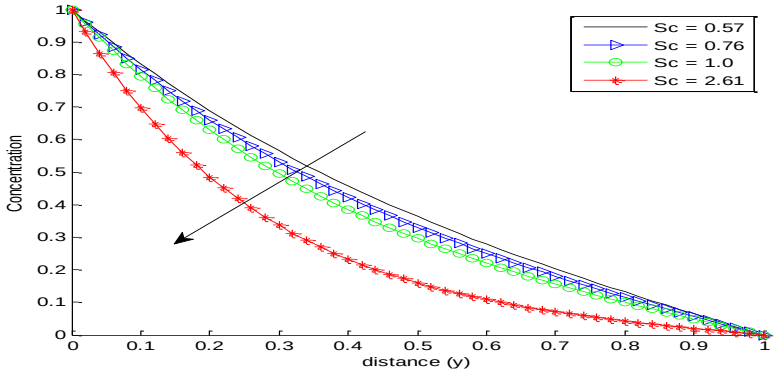

Figure 12: Effect of Schmidt number (Sc) on Concentration profile when M = 1, dt = 0.2, dy = 1/m, y = 0:dy:1, dy2 = 2.0*dy, Gr = 5, Gc = 5, R = 0.10, t = 0.2,Kr = 1 and Sc = 0.57.

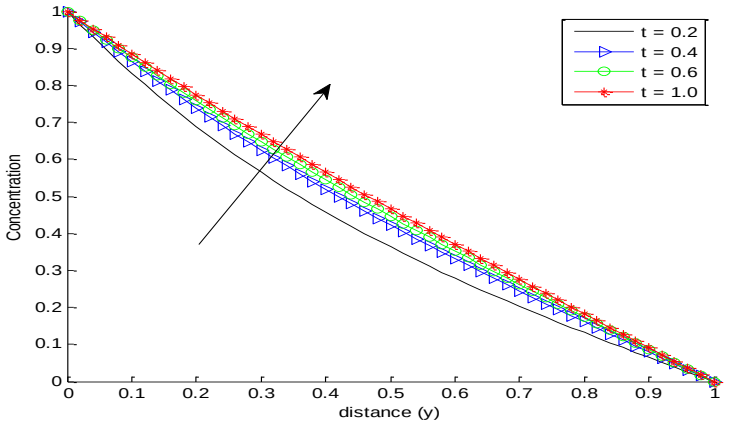

Figure 13: Effect of time (t) on Concentration profile when M = 1, dt = 0.2, dy = 1/m, y = 0:dy:1, dy2 = 2.0*dy, Gr = 5, Gc = 5, R = 0.10, Kr = 1 and Sc = 0.57.

It is noticeable in Figure 10, the graph depict that the temperature increases with an increase in the heat source parameter. This is due to the fact that more energy is being supplied to the system, causing its temperature to rise as a result of increased thermal energy input. This finding also corresponded to the result of Khan *et al.* (2022). Likewise, Figure 11 reveals that the fluid temperature increases whenever the time increases. Figure 12 illustrates the effect of the Schmidt number (Sc) on concentration. It is observed that the concentration decreases with an increase in the Schmidt number. As the Schmidt number increases, the fluid tends to transfer momentum more efficiently than mass (concentration). Consequently, this leads to a decrease in concentration because less mass is being effectively transferred through the fluid,

but the opposite phenomenon was observed in Figure 13, which shows that the concentration of the fluid increases with an increase in time.

CONCLUSION

This paper investigates a study on unsteady MHD-free convective flow past a vertical oscillating plate through a porous medium in the presence of a heat source. The velocity, temperature, and mass diffusion, which govern the flow, are solved by the implicit finite difference method. The effects of different parameters, namely the magnetic field parameter, radiation parameter, Grashof number, mass Grashof number, Prandtl number, Schmidt number, porosity parameter, and heat source parameter, were analyzed graphically. The conclusions of the study are as follows: It has been found that the velocity profile decelerates with an increase in the magnetic field parameter (M), Prandtl number (Pr), radiation parameter (R), permeability of porous medium (K), Schmidt number (Sc), and time (t), respectively. It is also observed that as the heat source parameter Q increases, the velocity of the fluid increases. Increasing values of Grashof number (Gr), Grashof number for mass transfer (Gm), porous medium parameter (K), and time (t) accelerate the fluid velocity. The analysis showed that increasing Prandtl number (Pr) decreases fluid temperature. Fluid temperature increases with increasing radiation parameters (R), heat source parameters (Q), and time (t). Concentration decreases with an increase in the Schmidt number Sc.

REFERENCES

Akcay, S., Akdag, U. and Palancioglu, H., (2020). Experimental investigation of mixed convection on an oscillating vertical flat plate. *International Communications in Heat and Mass Transfer,* 113, 104528.

Alwawi, F.A., Alkasasbeh, H.T., Rashad, A.M. and Idris, R., (2020). MHD natural convection of Sodium Alginate Casson nanofluid over a solid sphere. *Results in physics*, *16*, p.102818.

Amar, N., Kishan, N., Goud, B.S., (2022). MHD heat transfer flow over a moving wedge with convective boundary conditions with the influence of viscous dissipation and internal heat generation/absorption. *Heat Transfer,* 51(6), pp. 5015-5029.

Bafakeeh O. T., Raza A., Khan U. S., Khan M. I., Nasr A., Khedher N.B. and Tag- Eldin E.M. (2022). Physical interpretation of Nanofluid (Copper Oxide and Silver) with slip and mixed convection effects: Application of fractional derivatives; *Applied Sciences*, 12 (21), 10.3390/app122110860.

Bilal, S., Shah, I.A., Ghachem, K., Aydi, A. and Kolsi, L., (2023). Heat Transfer Enhancement of MHD Natural Convection in a Star-Shaped Enclosure, Using Heated Baffle and MWCNT–Water Nanofluid. *Mathematics*, *11*(8), p.1849. https://doi.org/10.3390/ math11081849.

Chitra M. and Suhasini M. (2018). Effect of unsteady oscillatory MHD flow through a porous medium in porous vertical channel with chemical reaction and concentration, *National Conference on Mathematical Techniques and its Applications,* 012039, doi :10.1088/1742-6596/1000/1/012039

Elbashbeshy E. M. A., H. G. Asker, and B. Nagy, (2022). The effects of heat generation absorption on boundary layer flow of a nanofluid containing gyrotactic microorganisms over an inclined stretching cylinder, *Ain Shams Engineering Journal*, 13(5), pp. 101690 doi: 10.1016/j.asej.2022.101690.

Fu, W.S. and Tong, B.H., (2017). Numerical investigation of heat transfer from a heated oscillating cylinder in a cross flow. *International Journal of Heat and Mass Transfer,* 45(14), pp.3033–3043.

Hartmann, J. and Lazarus, F. (1937). Hg-dynamics II: theory of laminar flow of electrically conductive liquids in a homogeneous magnetic field, *Matematisk-Fysiske Meddelelser*, 15(7).

Hussain, S.M., Goud, B.S., Madheshwaran, P., Jamshed, W., Pasha, A.A., Safdar, R., Arshad, M., Ibrahim, R.W., Ahmad, M.K., (2022). Effectiveness of Nonuniform Heat Generation (Sink) and Thermal Characterization of a Carreau Fluid Flowing across a Nonlinear Elongating Cylinder: A Numerical Study. *ACS Omega,* 7(29), pp. 25309–25320.

Jahangiri, M. and Delbari, O., (2020). Heat transfer correlation for two phase flow in a mixing tank. Journal of *Heat and Mass Transfer research,* 7(1), pp.1-10.

Jawad, M., Saeed, A. and Gul, T. (2021). Entropy generation for MHD Maxwell nanofluid flow past a porous and stretching surface with Dufour and Soret effects. *Brazilian. Journal of Physics,* pp. 1-13. Doi: 10.1007/s1353802000835-x

Khalid, A., Khan, I. and Shafie, S., (2017). Free convection flow of micropolar fluids over an Oscillating vertical plate. *Malaysian Journal of Fundamental Applied Science,* 13(4), pp.654–658.

Khan M., M. Yasir, A. Saleh, S. Sivasankaran, Y. Rajeh, and A. Ahmed, (2022). Variable heat source in stagnation-point unsteady flow of magnetized Oldroyd-B fluid with cubic autocatalysis chemical reaction, Ain *Shams Engineering Journal*, 13(3), pp. 101610 doi: 10.1016/j.asej.2021.10.005.

Krishna, M.V., Reddy, M.G., Chamkha, A.J., (2019). Heat and mass transfer on MHD flow over an infinite non-conducting vertical flat porous plate. *Journal of Porous Media,* 46 (1), pp. 1-25.

Muthucumaraswamy, R. and Ghetta E. (2013) Chemical Reaction Effects on MHD Flow Past a Linearly Accelerated Vertical Plate with Variable Temperature and Mass Diffusion in the Presence of Thermal Radiation, *International Journal of Applied Mechanics and Engineering*.vol.18, No.3, pp.727-737

Nemati M., M. Sefid, and A. R. Rahmati, (2021). Analysis of the Effect of Periodic Magnetic Field, Heat Absorption / Generation and Aspect Ratio of the Enclosure on Non-Newtonian Natural Convection, *Journal of Heat and Mass Transfer Research*,8, pp. 187–203 doi: 10.22075/JHMTR.2021.22119.1322.

Noor N. A. M., Shafie, S., and Admon, M. A. (2020). Unsteady MHD squeezing flow of Jeffrey fluid in a porous medium with thermal radiation, heat generation/absorption and chemical reaction. *Physica Script,* 95(10), 105213.

Pradhan, B., Das, S.S., Paul, A.K. and Dash, R.C., (2017). Unsteady free convection flow of a viscous incompressible polar fluid past a semi-infinite vertical porous moving plate. *International Journal of Applied Engineering Research,* 12(21), pp.10958–10963.

Pourgholam, M., Izadpanah, E., Motamedi, R. and Habibi, S.E., (2015). Convective heat transfer enhancement in a parallel plate channel by means of rotating or oscillating blade in the angular direction. *Applied Thermal Engineering,* 78(5), pp.248–257.

Rahman, A. and Tafti, D., (2020). Characterization of heat transfer enhancement for an oscillating flat plate-fin. *International Journal of Heat and Mass Transfer,* 147, 119001.

Sarhan, A.R., Karim, M.R., Kadhim, Z.K. and Naser, J., (2019). Experimental investigation on the effect of vertical vibration on thermal performances of rectangular flat plate. *Experimental Thermal and Fluid Science,* 101, pp.231–240.

Sharma T., Sharma P. and Kumar N. (2022). Study of dissipative MHD oscillatory unsteady free convective flow in a vertical channel occupied with the porous material in

the presence of heat source effect and thermal radiation, *International Symposium on Fluids and Thermal Engineering,* 012012. doi:10.1088/1742-6596/2178/1/012012.

Sheikholeslami M., (2022). Numerical investigation of solar system equipped with innovative turbulator and hybrid nanofluid, *Solar Energy Materials and Solar Cells*, 243, pp. 111786.

Usman H. and Sanusi S. (2023). Heat and mass transfer analysis for the mhd flow of Casson nanofluid in the presence of thermal radiation, *FUDMA Journal of Sciences* 7(2), pp 188 – 198. https:doi.org/10.33003/fjs-2023-0702-1728

Yasir M., A. Ahmed, M. Khan, Z. Iqbal, and M. Azam, (2022). Impact of ohmic heating on energy transport in double diffusive Oldroyd-B nanofluid flow induced by stretchable cylindrical surface, *Proceedings of the Institution of Mechanical Engineers, Part E: Journal of Process Mechanical Engineering*, 0(0) doi: 10.1177/09544089211064116.